Observation of Mix in a Compressible Plasma in a Convergent Cylindrical Geometry

Cris W. Barnes, S. H. Batha, A. M. Dunne*, G. R. Magelssen, Steve Rothman*, R. D. Day, N. E. Elliott, D. A. Haynes+, R. L. Holmes, J. M. Scott, D. L. Tubbs, D. L. Youngs*, T. R. Boehly**, P. Jaanimagi**

Los Alamos National Laboratory, Los Alamos, NM 87545 USA

**AWE Aldermaston, United Kingdom*

+University of Wisconsin, Madison, WI

***Laboratory for Laser Energetics, University of Rochester, Rochester, NY*

(Submitted to Physical Review Letters March 5, 2001; LA-UR-01-0994

Revised version February 8, 2002)

Laser beams that directly drive a cylindrical implosion are used to create a measurable region of mixed material in a compressible plasma state, for the first time in a convergent geometry. The turbulence driven by the Richtmyer-Meshkov instability by shock passage across a density discontinuity mixes marker material that is radiographically opaque. The width of the mix layer is compared between a system with large surface roughness and an initially smooth system. The experiment is described and results are compared to multi-dimensional direct numerical simulation, including three-dimensional turbulence calculations. The calculations adequately match the observations provided the measured initial conditions are used.

52.57.Fg,52.65.Kj,47.40.Nm

An interface between different materials suffers mix when it undergoes hydrodynamic instability from acceleration or passage of a shock. Such mixing is especially of interest in explosions or implosions including astrophysical problems [1] such as supernova or in fusion research using inertial confinement [2]. In these systems the turbulence is often inhomogeneous and anisotropic and the mix is between materials of different density. Furthermore, the energy densities in these systems is great enough to ionize the material into a plasma state and make the hydrodynamics compressible. Finally, such implosion systems are convergent, and the effects of the convergence on the physics of the mix are of interest. There is no accepted theoretical or computational model for explaining such complex environments, and experimental data in such regimes are needed.

We describe a mix experiment that creates a measurable region of mixed material in a compressible plasma state in a convergent cylindrical geometry. The turbulence is primarily driven by the passage of a single shock across a perturbed, variable density interface. Much previous work has been incompressible [3] or, if compressible, in planar geometry [4,5]. In contrast to the pioneering work on turbulent mix of Dimonte *et al.* [5] this work is convergent with corresponding effects expected on the hydrodynamics [6]. This experiment establishes a stringent test of mix modelling capability in a complex, inertial-fusion relevant environment.

The experiment uses directly driven cylindrical implosions [7,8] on the OMEGA laser [9] at the Laboratory for Laser Energetics of the University of Rochester. Thin-walled polystyrene cylinders 2.25-mm long and 0.86-mm inner diameter with 60-mg/cm^3 polystyrene foam inside are directly illuminated with 351-nm wavelength light from 50 laser beams in a 1-ns square laser pulse. The imploding cylinder is then radiographed with the x rays from a laser-heated titanium or iron foil normal to the cylinder along its axis. Use of the cylindrical geometry allows convergent interfaces to be observed directly from the side.

The entire cylinder implodes in an hour-glass shape from the variation in intensity along the axial direction. The mixing region is kept "one-dimensional" (initially dependent only on radius) by isolating the primary material interfaces along a thin 500-μm long "marker" region in the center of the cylinder where the laser drive is uniform. The marker material is chosen to be more opaque to the backlighter x rays and to have a different density from the ablator or foam. Two systems have been compared (Figure 1): a system that demonstrates the minimum marker extent achievable with no mix, using a smooth 4-μm thick poly(2,6-dichloro)styrene marker created by machining the styrene on an original aluminum mandrel; and the other a system that demonstrates mix, using 0.85 μm of gold deposited conformally on the central foam. The ablators are made thick, consisting of 73-μm polystyrene over the styrene marker or 60-μm polystyrene over the gold. This design choice matches the total mass between the systems, with the pusher thickness determined so that the shock breaks out from the pusher at the end of the laser pulse. The material interfaces are hydrodynamically unstable when accelerated, but the smooth initial amplitudes of the lower density styrene create little mix compared to the high initial amplitudes of the high density gold. The extent of the mixing of the materials across the interfaces is then measured.

Direct comparisons of the calculated hydrodynamics with experiment use the 2D Lagrangian hydrocode LASNEX [10] to calculate the axial implosion

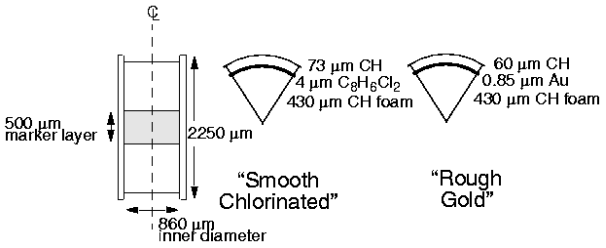

FIG. 1. r-Z and r-θ drawings of smooth chlorinated styrene and rough gold marker systems.

profile along the radial direction r and axial direction Z, and the 2D Eulerian hydrocode PETRA [11,12] to calculate the turbulent mixing in either the r-Z or r-θ planes (i.e. assuming symmetry in the azimuthal θ or axial z directions, respectively). The measured laser power and, for PETRA, the material interface roughness spectra are used. The calculations confirm that the laser-driven shock reaches the interface at 1 ns at the end of the laser pulse, leading to a minimal period of interface acceleration during the laser drive and thus miminizing Rayleigh-Taylor growth in the early stages. The mix comes primarily from single-shock Richtmyer-Meshkov turbulence at the pusher-foam interface. Mach numbers of the shock are calculated to be > 20, with Reynold's numbers in the post-shock marker layer $\sim 10^6$ [13].

Matching the marker layer to be the length of the uniform illumination region was predicted to keep the marker imploding rectilinearly until stagnation [7] and experimentally confirmed [8] in previous thin-ablator work. The LASNEX r-Z calculations also predict a suitable rectilinear shape of the polystyrene marker. However, the significantly greater radial line density through the gold marker layer relative to through the plain styrene causes a hydrodynamic mismatch at the ends of the marker. The plain ablator runs ahead of the marker, increases pressure inside the marker at its ends, and also drags the end of the marker inward, effectively increasing the apparent thickness of the marker when viewed axially. Figure 2 shows a simulated side-on radiograph just before turnaround. This type of "clean" calculation estimates that some but not all of the apparent "mix width" in the gold marker case may be caused by these effects.

As with previous R-M turbulence experiments [5], the initial conditions of the targets and the pusher-foam interfaces have been well characterized. Dimensions of the styrene marker layers were measured to be 3.9 ± 0.8 μm from scanning electron microscope (SEM) images. Other styrene dimensions were measured to better than 1-μm accuracy using optical microscopy or a laser micrometer. The gold was observed by SEM to lay conformally on the rough foam surface, and its thickness determined to

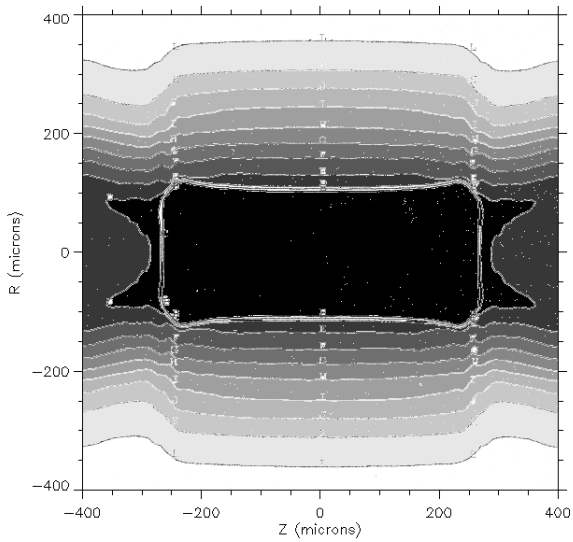

FIG. 2. Simulated r-Z radiograph of a smooth gold marker cylinder implosion at 4.75 ns using the LASNEX code. This is a "clean" calculation with no initial surface roughness on the gold layer.

be 0.85 ± 0.05 μm from two different techniques, x-ray radiography and x-ray fluorescence. The initial surface roughness of the interface was measured, the styrene by two optical interferometers and the gold by both the interferometers and by a laser confocal scanning microscope. Figure 3 illustrates the measurements of the surfaces and shows how the power per unit wavenumber of the surface roughness decreases with wavenumber k as $k^{-3/2}$ for the gold-on-foam and k^{-2} for the machined styrene. There are factors of two uncertainty in the initial amplitude of the rough foam surfaces arising from sample variations and different measurement techniques.

Shots typically had 19–20 kJ on target with better than 8% RMS energy balance. The laser beams were smoothed with distributed phase plates and two-dimensional smoothing by spectral dispersion (SSD) of 1.5Å$\times$3.0Å bandwidth. Rotational alignment of the cylinders to within ± 0.3 degrees and positional (XYZ) alignment to within ± 50 μm was achieved by careful pre-shot metrology using alignment fibers on the target. Targets were radiographed during 4.0–5.0 nsec, just prior to minimum radius. At this time the mix width is maximized while avoiding the period after shock reflection.

A variety of diagnostics monitored the implosions. A framing camera observed self-emission and confirmed correct target alignment. An imaging x-ray streak camera, with its slit across the radius, measured the time dependence of the self-emission and confirmed that the laser was not interacting with the marker layer unlike previous thin ablator experiments. X-ray spectroscopy (both streaked and time-

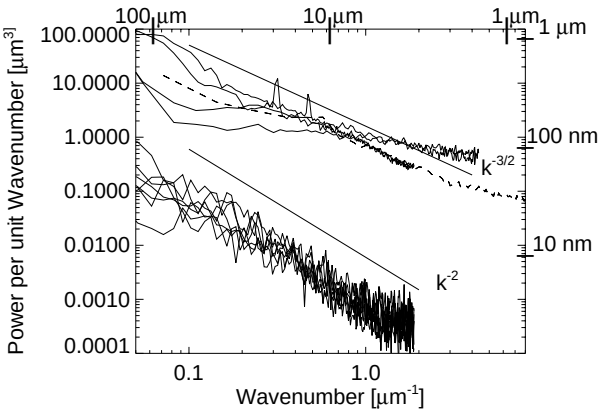

FIG. 3. Surface roughness of the pusher-foam interface. Plotted is the power (square of the amplitude) per unit wavenumber (dividing each measurement by its bandwidth dependent on the sample length). Data from the machined styrene (several traces at lower amplitude) and gold surfaces are shown from both optical interferometers on different samples (thin and thick lines), and confocal laser scanning microscope (dashed lines). The wavelength is shown on the top, and equivalent amplitude for the 500 μm marker shown on the right.

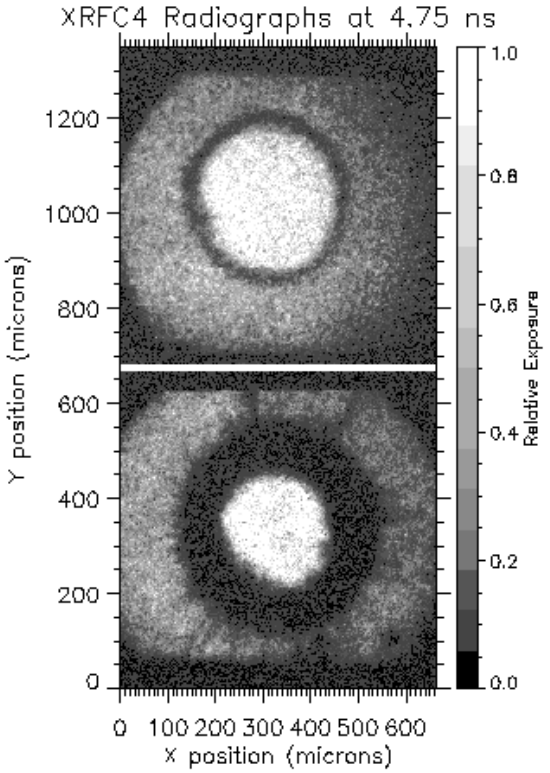

FIG. 4. Axial x-ray radiography of the imploding cylinders at the same time in their implosion (4.75 nsec). Top) Smooth chlorinated styrene marker case. Film exposure for this image with iron backlighter has been normalized to an average of 0.0145 erg/cm^2 in the center. Bottom) Rough gold marker case. Film exposure for this image with titanium backlighter has been normalized to an average of 0.0170 erg/cm^2 in the center.

integrated) also confirmed the absence of laser interaction with the chlorine or gold of the marker layers. The hot electron temperature can be characterized by the hard x-ray spectrum as being 10–15 keV; hence for these thick ablators there should be no significant preheat of the marker layer by hot electrons. The backlighter x-ray spatial profile was found to be represented by a Gaussian [8].

Figure 4 shows typical axial radiographs for both styrene and gold marker cases. The frames are chosen to be at the same time (4.75$\pm$0.10 ns) during the respective implosions which had incident laser energy within 1.4% of each other. The fundamental result of this work is that we see a relatively thin marker layer with the initially smooth, chlorinated system but a very thick mix region with the initially rough, gold system.

Hydrodynamic instabilities at the marker-foam interface are certainly seeded and develop fully in three dimensions. However, the diagnostic line-of-sight along the axis integrates through the system and creates an image as though looking at a two-dimensional r-θ system. The experiments are explicitly modelled using both 2D and 3D hydrocodes to predict the plasma turbulence and material interpenetration. The TURMOIL fluid code [14] (using an ideal gas approximation and a pressure boundary condition obtained from the 2D results) show that differences between 2D and 3D growth are minor, but indicate that 3D effects at the end of the marker layer may extend the apparent outer edge of the transmission profile by 10–20 μm. The 2D PETRA r-θ and r-Z calculations predict quantitatively similar mix distributions. The r-Z calculations which include the effects on transmission from ablator material at the ends are thus used to provide a direct comparison with the data, using IMP opacities [15] to generate a simulated radiograph, which is then convolved with the measured backlighter spatial profile. Figure 5 shows a comparison of the calculated mix profile and data obtained in the rough gold marker implosion. Also shown is the transmission profile from a "clean" LASNEX 2D simulation that assumes no surface roughness, which illustrates the expected marker width from zeroth-order hydro with no turbulent mix and which is much smaller than measured. LASNEX uses our best simulation of laser deposition with as-shot laser energy and profile; however, these r-Z calculations overpredict the experimental implosion velocity and as shown in the Figure predict a smaller radius at the time of the measurement. Calculations done in r-θ match the measured zeroth-order hydro; we do not understand this issue with the r-Z calculations. The PETRA r-Z direct numerical simulation (DNS) calculation with surface roughness has had the incident

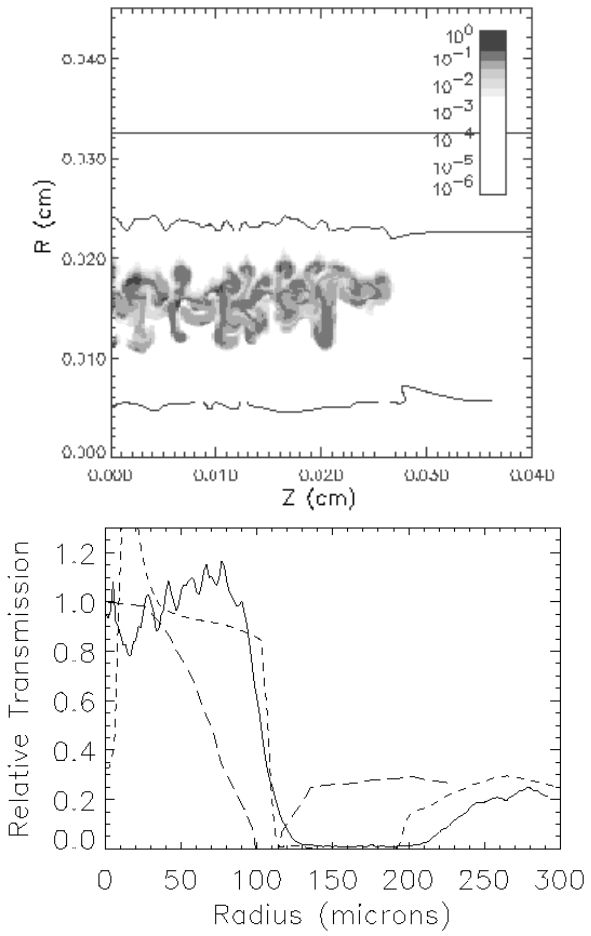

FIG. 5. Comparison of numerical simulations to experiment. Top) DNS calculation of gold volume fraction in rough gold marker case using r-Z PETRA simulation, at 4.75 ns. Bottom) Radial lineout of azimuthal average of relative transmission. The solid curve is the gold marker data at 4.75 ns, the short dashed line from the r-Z PETRA simulation above, and the long dashed line from the r-Z LASNEX simulation of a smooth gold marker of Fig. 2.

energy reduced by 7% so as to match the measured convergence of the experiment and the r-θ calculations. The relative transmission profile shows good quantitative agreement, especially in the location of the edges and hence the overall width of the mix layer. Experimental results from the styrene marker case are also in agreement with DNS calculations which show the styrene marker width is dominated by end effects and not mix.

We have studied the sensitivity of the results to variations in the experimental parameters and to code settings. Comparison with notional, hydrodynamically equivalent planar and cylindrical analogues demonstrate that convergence enhances the mix growth, by typically 20% over a planar case. The Atwood number, a dimensionless measure of the density jump across a material interface, is ill-defined in such a compressible system with significant density gradients and two interacting turbulent interfaces. DNS calculations comparing chlorine and gold marker layers of the same thickness and *same* initial roughness do predict a factor-2 less mix width from the lower density material. Uncertainties in the initial conditions (resulting from measurement inaccuracies, target variations, and minor preheat effects) are estimated to be less than a factor-of-2 in the surface roughness, which corresponds to less than 10% uncertainty in the predicted mix width.

In conclusion, this experiment demonstrates the ability to perform quantitative measurements of mix in convergent geometry using compressible plasmas. It provides a well-posed test of an integrated modelling capability, and explicit calculations using hydrocodes including fully 3D ones adequately match the observations provided proper initial conditions are used. These results act as the basis for generating 1D mix 'models' [14] which capture the essential growth characteristics and permit capsule optimization studies for ICF research in a convergent, compressible plasma environment rather than the usual incompressible fluid limit.

[1] D. Arnett, Astrophysical Journal Supplement Series **127**, 213 (2000).

[2] J. Lindl, Phys. Plasmas **2**, 3933 (1995).

[3] P. M. Rightley, P. Vorobieff, and R. F. Benjamin, Phys. Fluids **9**, 1770 (1997); M. B. Schneider, G. Dimonte, and B. Remington, Phys. Rev. Lett. **80**, 3507 (1998); S. T. Weir, E. A. Chandler, and B. T. Goodwin, Phys. Rev. Lett. **80**, 3763 (1998).

[4] G. Dimonte and B. Remington, Phys. Rev. Lett. **70**, 1806 (1993); T. A. Peyser, P. L. Miller, P. E. Stry, K. S. Budil, E. W. Burke, D. A. Wojtowicz, D. L. Griswold, B. A. Hammel, and D. W. Phillion, Phys. Rev. Lett. **75**, 2332 (1995); G. Jourdan, L. Houas, and M. Billiotte, Phys. Rev. Lett. **78**, 452 (1997).

[5] G. Dimonte, C. E. Frerking, and M. Schneider, Phys. Rev. Lett. **74**, 4855 (1995); G. Dimonte and M. Schneider, Phys. Plasmas **4**, 4347 (1997).

[6] G. I. Bell, Taylor instability on cylinders and spheres in the small amplitude approximation, Technical Report LA-1321, Los Alamos Scientific Laboratory, 1951; M. S. Plesset, J. Appl. Phys. **25**, 96 (1954).

[7] D. L. Tubbs, C. W. Barnes, J. B. Beck, N. M. Hoffman, J. A. Oertel, R. G. Watt, T. Boehly, D. Bradley, and J. Knauer, Laser Part. Beams **17**, 437 (1999); D. L. Tubbs, C. W. Barnes, J. B. Beck, N. M. Hoffman, J. A. Oertel, R. G. Watt, T. Boehly, D. Bradley, P. Jaanimagi, and J. Knauer, Phys. Plasmas **6**, 2095 (1999).

[8] C. W. Barnes, D. L. Tubbs, J. B. Beck, N. M. Hoffman, K. A. Klare, J. A. Oertel, R. G. Watt, T. R. Boehly, D. K. Bradley, and J. P. Knauer, Rev. Sci. Instrum.

70, 471 (1999).
[9] T. R. Boehly, D. L. Brown, R. S. Craxton, R. L. Keck, J. P. Knauer, J. H. Kelly, T. J. Kessler, S. A. Kumpan, S. J. Loucks, S. A. Letzring, F. J. Marshall, R. L. McCrory, S. F. B. Morse, W. Seka, J. M. Soures, and C. P. Verdon, Optics Communications **133**, 495 (1997).
[10] G. B. Zimmerman and W. L. Kruer, Comments Plas. Phys **2**, 51 (1975).
[11] D. L. Youngs, Time-dependent multi-material flow with large fluid distortion, in *Numerical Methods for Fluid Dynamics*, edited by K. W. Morton and M. J. Baines, Academic Press, London, 1982.
[12] D. L. Youngs, Physica **12D**, 32 (1984).
[13] D. Galmiche and S. Gauthier, Jpn. J. Appl. Phys. **X**, Part 1, No. 8, 4516 (2001).
[14] D. L. Youngs, Laser Part. Beams **12**, 725 (1994).
[15] S. J. Rose, J. Phys. B **25**, 1667 (1992).